Prolonged Lifetime of the Transient Ionized Layer in the Martian Atmosphere Caused by Comet Siding Spring

Z. A. Luppen[1], **Z. Girazian**[1], **D. D. Morgan**[1], **A. J. Kopf**[1], **F. Chu**[1], **J. S. Halekas**[1], **D. A. Gurnett**[1]

[1]Department of Physics and Astronomy, University of Iowa, Iowa City, Iowa, USA

Key Points:

- The transient ionospheric layer at Mars caused by comet Siding Spring's flyby may have lasted at least 7 days, and up to 32 days.
- All detected transient layer measurements were located between 20°N-60°N latitude, and most were confined to one longitudinal hemisphere.
- We discuss how solar flares may have contributed to the prolonged lifetime of the transient layer.

Corresponding author: Zachary Luppen, `zaluppen@iastate.edu`

Abstract

In October 2014, the close encounter between Mars and comet Siding Spring produced a transient ionized layer in the upper atmosphere composed primarily of Mg^+ ions. The layer was detected by instruments on three spacecraft, including the Mars Advanced Radar for Subsurface and Ionosphere Sounding (MARSIS) on Mars Express. Analyses of the MARSIS data indicated the transient layer persisted up to ~19 hours after the comet's closest approach. We report MARSIS observations that suggest the transient layer lasted at least 7 days – and potentially as long as 32 days – after closest approach. During this period, the transient layer was mostly confined to a narrow latitude range between 20°N-60°N and a longitude range spanning 275°E to 95°E. Since this period coincided with a highly active Sun, we discuss how solar flares may have contributed to the layer's prolonged lifetime.

1 Introduction

On 19 October 2014, at 18:29 UT, comet Siding Spring (C/2013 A1) flew close to Mars, passing within 40 Mars radii along a highly-inclined orbital path. The event presented a rare opportunity to understand how cometary material is deposited and distributed in the Martian upper atmosphere, and to test models of metal ion chemistry. During the close flyby, 82 (±25) tons of cometary material was deposited into the upper atmosphere of Mars with an approach velocity of 56 km s^{-1} [*Crismani et al.*, 2018]. Upon entry, the ablated material deposited an abundance of metallic species such as Mg, Na, and Fe into the upper atmosphere [*Benna et al.*, 2015; *Schneider et al.*, 2015; *Crismani et al.*, 2018]. The material formed a transient ionized layer with a peak altitude near 115 km that was detected by instruments on multiple spacecraft. This layer, composed primarily of Mg^+ ions, was produced by the ionization of ablated material through collisions, photoionization, and charge exchange with existing ionospheric ions [*Whalley and Plane*, 2010; *Crismani et al.*, 2018; *Plane et al.*, 2018].

Within 10 hours after the comet's closest approach (Δt_{ca} = 10 hours), the Mars SHAllow RADar sounder (SHARAD) on the Mars Reconnaissance orbiter (MRO) detected the transient ionized layer during two MRO orbits. Both of the observations, from the nightside of the planet, showed an exceptional increase in the nightside total electron content (TEC) that was attributed to ablated cometary material [*Restano et al.*, 2015].

The Mars Atmosphere and Volatile EvolutioN (MAVEN) spacecraft, which had just reached Mars in late September 2014, was in a limited powered-on state to collect data during the event. In situ measurements by MAVEN's Neutral Gas and Ion Mass Spectrometer (NGIMS) showed an abrupt increase in Mg^+, Na^+, Fe^+, and other metallic ion species during its first observations on 20 October ($\Delta t_{ca} \simeq$ 10 hours) [*Benna et al.*, 2015]. The metal ions were continuously detected until periapse observations ceased on 22 October ($\Delta t_{ca} \simeq$ 2.5 days). *Benna et al.* [2015] also reported that the Mg^+ abundance at 185 km decayed with an e-folding timescale of ~8 days, much longer than the 1.8 days predicted by a 1-D chemical model [*Whalley and Plane*, 2010]. This discrepancy was attributed to the rapid transport of metallic ions by thermospheric winds, which were not included in the 1-D model.

During the flyby, periapse limb scans from MAVEN's Imaging Ultraviolet Spectrograph (IUVS) between 50°N and 5°S measured Mg^+ and Fe^+ transient layer altitude profiles [*Crismani et al.*, 2018]. The observations showed that the transient layer was primarily composed of Mg^+, with a peak density of as much as 2×10^5 cm^{-3}, and a peak altitude near 115 km [*Schneider et al.*, 2015; *Crismani et al.*, 2018]. These results also indicated that ablation occurred on a timescale less than 4.5 hr, primarily impacting only one hemisphere of Mars between ~50°E and ~230°E longitude (see Figure 1) [*Crismani et al.*, 2018]. Hours after closest approach, the metallic species were observed globally, including on the unexposed hemisphere, once again implying that they were transported across the planet by thermospheric winds.

Figure 1, adapted from Figure 9 in *Crismani et al.* [2018], shows the IUVS observations from 20-21 October ($\Delta t_{ca} \simeq$ 1.0-2.5 days). These IUVS limb scans measure ultraviolet emissions, which can be converted into altitude profiles of the Mg^+ and Fe^+ densities. During orbits 121-122, the transient layer was confined to a narrow latitude range between 20°N-60°N. The highest densities were observed near a region of the exposed hemisphere spanning ~90° between 300°E and 30°E longitude during MAVEN orbits 121 and 122 (shaded region, Figure 1). These measurements taken several days after closest approach are peculiar, and hint at a transport mechanism that confines metal ions to specific locations. Such a mechanism has yet to be determined, although *Crismani et al.* [2017] suggested global circulation patterns or crustal magnetic fields may play a role.

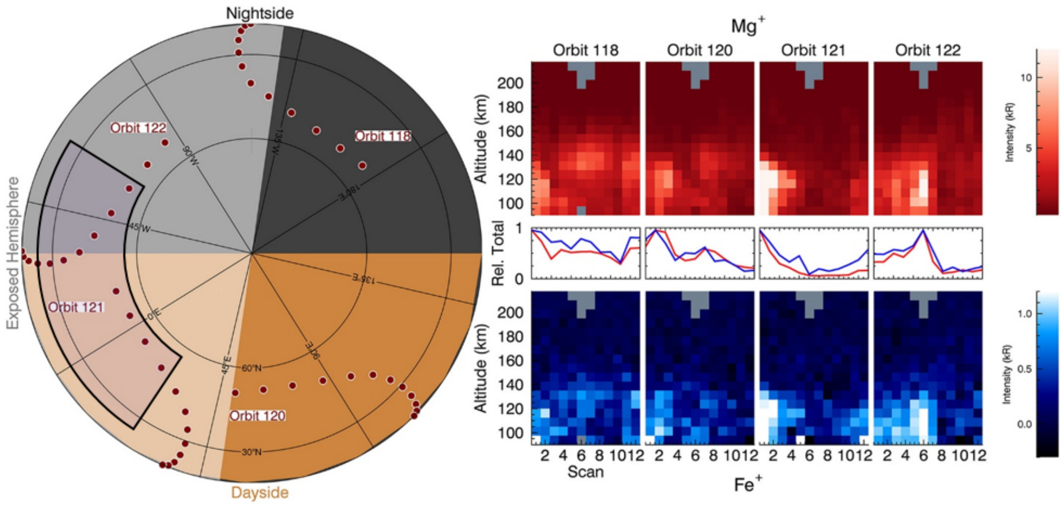

Figure 1. MAVEN IUVS observations of the transient ionized layer caused by comet Siding Spring. The observations range from 20-21 October, covering 1.0-2.5 days after the comet's closest approach. The observational geometry on the left side of the figure shows the location of each IUVS limb scan. For each orbit, the scans move consecutively from north to south and west to east. The Mg^+ and Fe^+ emissions observed during the limb scans are shown on the right side. Localized, bright emissions indicate the metal ions were patchy and variable throughout the upper atmosphere. The locations of these localized emissions during orbits 121-122 are marked with a shaded region. This figure is adapted from Figure 9 of *Crismani et al.* [2018].

The Mars Advanced Radar for Subsurface and Ionosphere Sounding (MARSIS) on Mars Express (MEX) also detected the transient layer on both the dayside and nightside up to $\Delta t_{ca} \simeq$ 19 hours [*Gurnett et al.*, 2015; *Venkateswara Rao et al.*, 2016]. The maximum observed peak electron density of 2×10^5 cm^{-3} was consistent with the IUVS observations [*Gurnett et al.*, 2015; *Venkateswara Rao et al.*, 2016; *Crismani et al.*, 2018]. Although the reported peak altitude of the transient layer by MARSIS was 100 ± 7 km [*Gurnett et al.*, 2015], improved data processing techniques by the MARSIS team later showed that the observed peak altitude was 113±7 km, much more consistent with the IUVS observations.

Despite these observations and analyses, there are still unanswered questions in regards to the chemistry and dynamics of the metal ions in the upper atmosphere of Mars. To date, models have been unable to reproduce the behavior of metal ions following Siding Spring's closest approach [*Benna et al.*, 2015; *Crismani et al.*, 2018]. One reason for this is that the models thus far do not include winds, which can transport the metal species to locations far from where they were created. Moreover, although it is generally accepted that metal ions have long chemical lifetimes of days or even weeks, their chemical lifetimes are poorly constrained by direct observations [*Crismani et al.*, 2017; *Grebowsky et al.*, 2017].

In this paper, we further analyze MARSIS data to look for transient layer detections up to a month after Siding Spring's closest approach. About 2.5 days after closest approach, MAVEN ceased normal science operations for several weeks, making MARSIS one of the only instruments able to monitor the ionosphere during this time. MARSIS is a topside sounder that can only measure electron density and cannot discriminate between different ions [*Gurnett et al.*, 2015]. Thus, we cannot definitively prove that we observe the Mg^+ layer. Nonetheless, we present peculiar MARSIS observations after the comet's closest approach that suggest the transient Mg^+ layer lasted for at least 7 days.

It is also worth noting that Siding Spring's encounter with Mars coincided with a period of strong space weather. Two days prior to closest approach, Mars encountered an interplanetary coronal mass ejection (ICME) which was detected by MEX, MAVEN, Mars Odyssey, and the Mars Science Laboratory [*Witasse et al.*, 2017]. These instruments indicated an increase in the solar wind density by a factor of ~2 as well as an increase in solar wind velocity, from ~400 km/s to ~700 km/s [*Witasse et al.*, 2017]. *Sánchez-Cano et al.* [2020] discussed how, before and during closest approach, the ionosphere was unusually variable, likely due to combined effects of the comet flyby and strong space weather [*Espley et al.*, 2015]. *Sánchez-Cano et al.* [2018] noted an increase in solar wind speed at Mars lasted from October 17-22. While the comet's closest approach to Mars was during this period, our key follow-up measurements on October 26 that we discuss are not. In Section 4, we discuss the potential effects of space weather on our measurements.

2 MARSIS Observations of the Transient Layer

2.1 The MARSIS Instrument

MEX is in a ~7 hour, near-polar orbit with an inclination of 86°. The orbit is highly elliptical, with an apoapsis altitude near 10,000 km, and a periapsis altitude near 375 km. During the periapsis portion of the orbit, when MEX is below ~1500 km, MARSIS conducts radar soundings using two 20 meter antennas, operating in one of two different observing modes: one for sounding the subsurface of Mars, and one for sounding the ionosphere [*Picardi et al.*, 2004]. In the Active Ionospheric Sounding (AIS) mode, the MARSIS transmitter emits radio pulses at frequencies between 0.1-5.4 MHz, and then measures the intensities and time delays of the return echoes – radio pulses that have been reflected off the ionosphere below ~250 km. Each frequency sweep takes 1.26 seconds and the entire process is repeated every 7.54 seconds.

The main data products produced by MARSIS soundings are ionograms – color-coded plots of the return echo intensities as a function of frequency and time delay [*Gurnett et al.*, 2005, 2008]. The time delay of each return echo provides information about its reflection altitude, with longer time delays indicating a lower altitude of reflection. The frequency of each return echo is a measure of the electron density at the reflection altitude, because radio waves are reflected when the local electron plasma frequency is equivalent to that of the MARSIS signal. For an extensive discussion of the MARSIS ionospheric sounding in context of the Siding Spring encounter, we refer the reader to *Gurnett et al.* [2015] and its supplementary material.

2.2 Identifying the Transient Layer in MARSIS Ionograms

2.2.1 Observations shortly before and after closest approach

Figure 2a shows an ionogram from 17 October 2014, two days before Siding Spring's closest approach. The ionogram has a clear ionospheric trace that is typical for observations of the dayside ionosphere far from appreciable crustal magnetic fields [*Gurnett et al.*, 2005, 2008]. The ionospheric trace is the thin line extending from 1.0-2.8 MHz whose time delay gradually increases with frequency. The time delay increases with frequency because, in the topside ionosphere, the electron density generally increases exponentially towards lower altitudes until the altitude of the main peak. The abrupt end of the ionospheric trace at ~2.8 MHz represents the reflection from the main peak of the ionosphere. Given the equation for the electron plasma frequency, $f_p = 8980\sqrt{N_e}$ Hz, where N_e is the electron density in cm^{-3}, this indicates a peak electron density of 9.7 x 10^4 cm^{-3}. Note that because MARSIS is a topside sounder, it cannot observe below the main peak of the ionosphere unless there is an additional layer there whose peak density exceeds that of the main peak. In addition to the ionospheric trace, the surface reflection trace is also present in Figure 2a, appearing as an approximately flat line between 3.2-5.5 MHz.

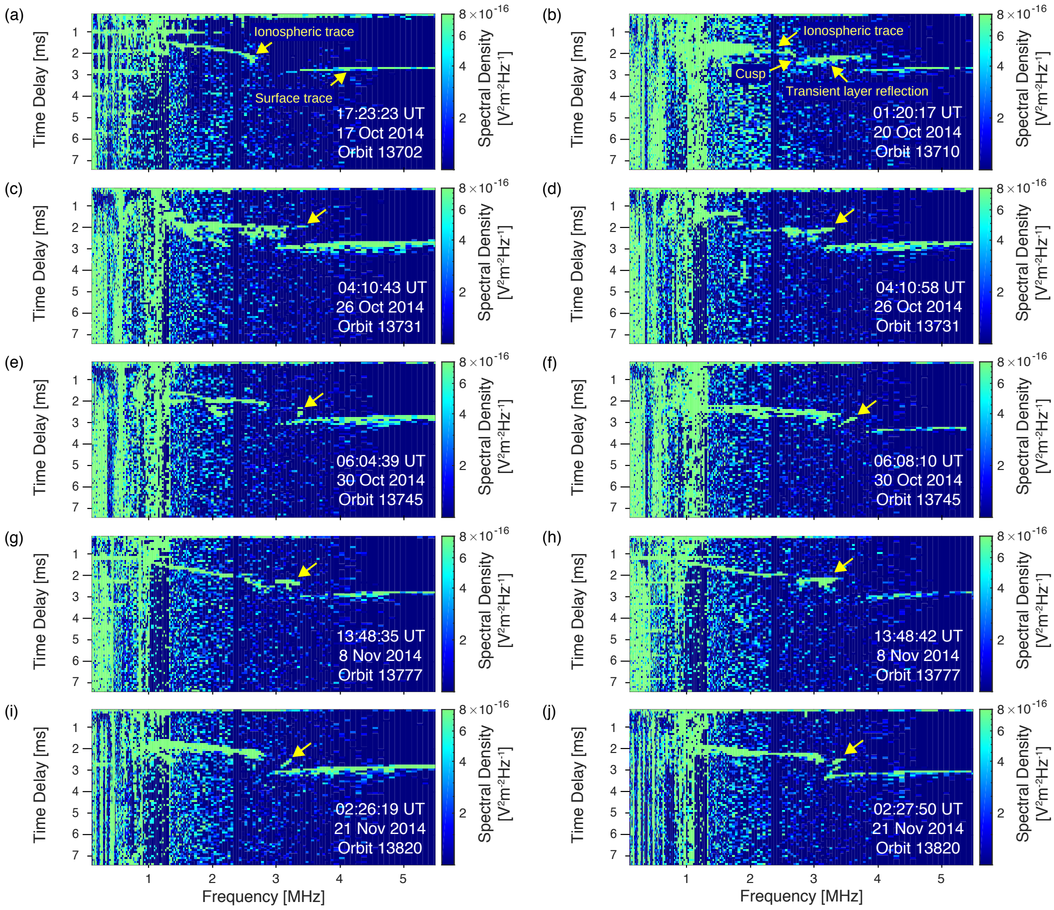

Figure 2. (a) A dayside ionogram with a typical ionospheric trace and a typical surface trace. (b) An ionogram from shortly after Siding Spring's closest approach ($\Delta t_{ca} \simeq 7$ hours) showing the reflection of the transient Mg^+ layer produced by the deposition of cometary material. (c-j) Eight ionograms with transient layer reflections (arrows) that we identified using the method explained in the text. The dates of the transient layer detections range from 26 October - 21 November ($\Delta t_{ca} \simeq$ 7-32 days).

Figure 2b shows an ionogram from 20 October 2014, shortly after Siding Spring's closest approach ($\Delta t_{ca} \simeq 5$ hours). The ionospheric trace is present, and there is an additional distinct feature between 2.8-3.8 MHz that is not present in the typical ionogram shown in Figure 2a. Based on its unique shape and extension to high frequencies, this feature has been identified as the Mg^+ transient layer reflection [*Gurnett et al.*, 2015; *Venkateswara Rao et al.*, 2016; *Crismani et al.*, 2018]. Unlike a typical ionospheric trace, the time delay of the transient layer reflection decreases with frequency, suggesting that there is a "cusp" between the ionospheric trace and the transient layer reflection. A cusp is a discontinuity in the trace that occurs when there is a local maximum in the electron density, such as at the main peak of the ionosphere [*Gurnett et al.*, 2008; *Kopf et al.*, 2008]. The presence of the cusp implies a non-monotonic variation in the electron density with altitude, i.e., the transient layer lies below the main peak of the ionosphere, and has a larger peak density than the main peak [*Gurnett et al.*, 2008; *Kopf et al.*, 2008; *Wang et al.*, 2009]. This is consistent with the MAVEN IUVS observations around the same time which observed the Mg^+ peak around 115 km [*Crismani et al.*, 2018]. The maximum frequency of the transient layer reflection is ~3.8 MHz, which corresponds to an electron density of ~1.8 x 10^5 cm^{-3}, one of the highest densities ever observed by the MARSIS instrument. The transient layer reflection appears in many ionograms throughout MEX orbits 13,710 and 13,711 which cover ~15 hours after closest approach [*Gurnett et al.*, 2015; *Venkateswara Rao et al.*, 2016].

The transient layer in Figure 2b overlaps the surface trace. The overlap indicates that at least some of the transient layer reflections are off-nadir [*Duru et al.*, 2010]. The presence of such off-nadir or oblique echoes implies strong horizontal gradients, or patchiness, in the ionosphere [*Duru et al.*, 2010; *Gurnett et al.*, 2015]. This patchiness of the transient layer is expected, given the localized regions of enhanced Mg^+ observed by MAVEN IUVS (Figure 1).

We must be cautious when interpreting oblique echoes, as they are sometimes observed near the terminator between 85°-95° SZA due to a strong day-to-night gradient in the ionospheric plasma density [*Duru et al.*, 2010]. However, since most of our observations have SZA less than 85°, this is unlikely to be a cause of the oblique echoes we observe. Additionally, oblique echoes and abnormally high peak densities are commonly observed near strong, vertical crustal magnetic fields [*Gurnett et al.*, 2008; *Fallows et al.*, 2019]. However, we show in Section 3 that all of our observations are obtained at northern mid-latitudes (45°N) far from any substantial crustal magnetism. Thus, it is unlikely that crustal magnetic fields are the primary cause of the oblique echoes we observe.

2.2.2 Observations more than one day after closest approach

Studies of MARSIS ionograms to date have detected the transient layer only up to MEX orbit 13,712 ($\Delta t_{ca} \simeq 19$ hours) [*Gurnett et al.*, 2015; *Venkateswara Rao et al.*, 2016]. To determine if the layer lasted longer, we search for transient layer reflections in dayside (solar zenith angle (SZA) < 90°) ionograms that were obtained up to a month after closest approach.

To identify transient layer reflections, we search by eye for ionospheric traces that either overlap the ground trace, or appear similar to the transient reflection shown in 2b. The former would indicate an oblique echo as discussed above [*Duru et al.*, 2008] and the latter serves as a good benchmark for interpreting distinct ionograms associated with Siding Spring. This simple visual analysis is typical for studying MARSIS ionograms [*Gurnett et al.*, 2008; *Morgan et al.*, 2008]. We exclude ionograms that are excessively noisy or that have obvious features caused by crustal magnetic fields [*Gurnett et al.*, 2008]. We extract the peak density from each transient layer using in-house software that identifies the highest frequency of a trace, and converts it into an electron density as described in *Morgan et al.* [2008]. Eight examples of transient layer reflections we identified are shown in Figures 2c-j.

Figures 2c-d show ionograms from 26 October 2014, seven days after closest approach. In both examples there is no discernible cusp at the end of the ionospheric trace. Instead, the trace extends to high frequencies that overlap the ground trace. The highest frequencies of the trace in Figure 2c, 3.5 MHz, correspond to a peak electron density of 1.5 $\times 10^5$ cm^{-3}. These peak densities are much larger than expected for the main peak of the ionosphere at a SZA near 77°, where the peak density is typically on the order of 1.0×10^5 cm^{-3} [*Morgan et al.*, 2008; *Withers*, 2009]. Furthermore, the trace shown in Figure 2d looks similar to the transient layer reflection observed shortly after closest approach (Figure 2b), with the time delay decreasing with frequency. Note, however, that both of these examples lack a cusp that is expected to be visible at the frequency corresponding to the main peak density as in Figure 2a-b. The lack of any cusp may suggest that the transient layer peak has moved upward and nearly merged with the main peak of the ionosphere.

Figures 2e-f show ionograms from 30 October 2014, eleven days after closest approach. Figure 2e has a small plasma feature at 3.4 MHz that overlaps the ground trace. This feature is well-separated from the ionospheric trace. Figure 2f shows a plasma feature at the high-frequency portion of the ionospheric trace. This feature appears similar to Figure 2d, with no discernible cusp and a time delay that decreases with frequency.

Ionograms shown in Figures 2g-j demonstrate that these unique trace features are still detectable until 21 November 2014, 32 days after Siding Spring's closest approach. After this date, we do not find any more ionograms with convincing features as those explained above. In total, we identify 86 ionograms with unusual features such as these. Characteristics of the 86 ionograms containing these features are listed in Table 1. We interpret these unusual features as being detections of the transient layer produced by Siding Spring's close flyby. In the next section, we show that the locations and peak densities of the transient layer measurements are consistent with the IUVS observations obtained shortly after closest approach.

3 Transient Layer Locations and Peak Densities

Figure 3 shows the latitudes and longitudes of all dayside MARSIS ionograms obtained between 19 October and 21 November in 2014. Ionograms with transient layer detections are colored according to Δt_{ca}, the number of days since closest approach. A map of the Martian crustal magnetic field strength at 400 km [*Morschhauser et al.*, 2014] is also shown. Most of the transient layer detections are located in weak crustal field regions where the field strength at 400 km is less than 10 nT (Table 1). Oblique echoes and unusually high peak electron densities, are much more commonly observed near radial crustal fields with an elevation angle (the angle between the magnetic field and the vertical) of less than 30° [*Gurnett et al.*, 2008]. Of the 86 transient layer detections used in this study, 55 have an elevation angle greater than 30° (Table 1), so crustal magnetic fields likely have minor effects on the measurements.

Although the MARSIS observations cover latitudes between 0°N-65°N, the detections are confined to a narrow range between 20°N-60°N. They are also non-uniformly distributed in longitude, with only 9 of the 86 transient layer detections between 95°E-275°E. This suggests the transient layer is mostly confined to one longitudinal hemisphere. Additionally, 63 of the 86 transient layer detections are between 280°E-45°E, which is near the locations where IUVS observed large amounts of Mg^+. In particular, the localized, bright Mg^+ measurements in scans 1-2 of orbit 121, and scans 5-6 of orbit 122, nearly coincide with the locations of our transient layer detections, even weeks after closest approach.

Figure 4 shows peak densities as a function of SZA using the same data. Each panel shows a different time range after closest approach. The gray points are the peak densities from ionograms that had normal ionospheric traces. The gray shaded regions encompass the 3σ standard deviations of the peak densities calculated using 2° SZA bins. For comparison, the peak densities of the transient layer detections are shown using red crosses.

The peak densities from October 19-22 ($\Delta t_{ca} \simeq$ 0-3 days) are shown in Figure 4a. The transient layer peak densities lie well above the 3σ envelope, indicating they are significantly larger than expected for the main peak of the ionosphere. The two groups of elevated transient layer peak densities near SZA=77° and SZA=85° are consistent with the transient layer peak densities reported in *Gurnett et al.* [2015].

The peak density measurements from October 23-25 ($\Delta t_{ca} \simeq$ 4-6 days) are shown in Figure 4b. The MARSIS coverage during this time period is highlighted in Figure 3 with

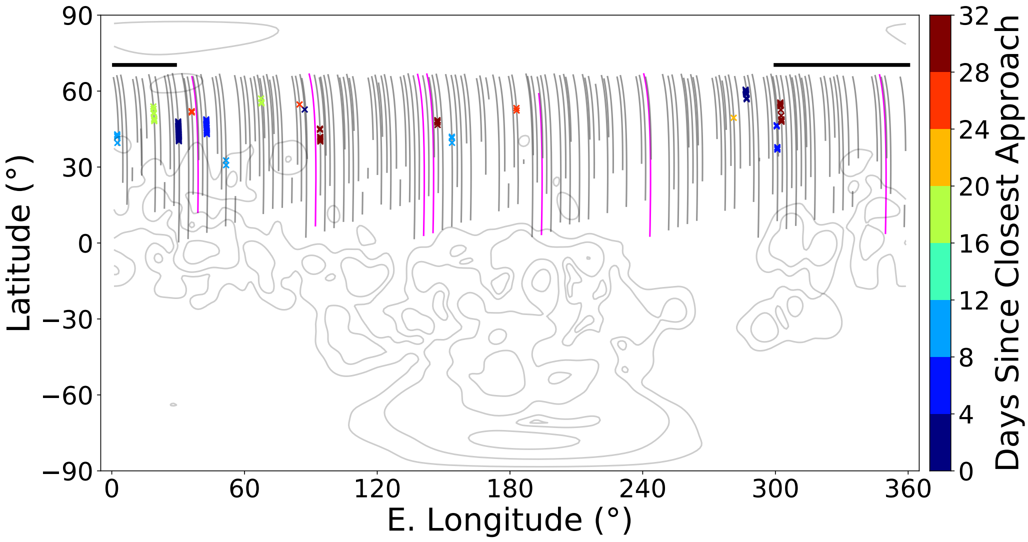

Figure 3. MARSIS observational coverage during 20 October - 21 November. The contours map the crustal magnetic field strength at 400 km [*Morschhauser et al.*, 2014]. The straight gray lines show all nominal MARSIS ionospheric measurements. The crosses mark the locations of transient layer detections we identified, colored according to days since closest approach. The pink lines show the coverage between 23-25 October, when we did not detect the transient layer (Fig. 4b). The black line above the data indicates the longitudes at which MAVEN's IUVS instrument detected localized, bright emissions 1.0-2.5 days after closest approach (see Figure 1).

pink lines. Despite MEX having similar orbital coverage (Fig. 3), we do not identify any transient layer reflections during this period. One orbit in particular, orbit 13,724, even covered nearly the same longitudes (E. Lon ≃ 40°) as orbit 13,710 (E. Lon ≃ 30°), when MARSIS readily observed the transient layer shortly after closest approach (Fig. 2b).

We again identify the transient layer beginning on 26 October ($\Delta t_{ca} \simeq 7$ days), as shown in Figure 4c. The SZAs of the transient layer measurements are similar to those detected shortly after closest approach (Fig. 4a). The transient layer peak densities are smaller than before, but mostly still lie above the 3σ envelope. The smaller peak densities suggest that the transient layer peak density decayed over time.

The peak densities from 29 October - 21 November ($\Delta t_{ca} \simeq$ 10-32 days) are shown in Figures 4d-f. We identify the transient layer during these three periods, at similar SZA ranges between 65°-85°. During all three of these periods, the transient layer peak densities are less significant outliers than before, suggesting that the transient layer continues to decay.

4 Discussion

Since MARSIS is a topside sounder that is unable to discriminate between different ions, we cannot be certain that the unusual features we identified in MARSIS ionograms are produced by reflections from the transient Mg^+ layer. Nevertheless, as described below, several aspects of our transient layer detections are consistent with expectations for this layer.

As described in Section 2, the transient layer reflections we identified between 26-28 October (Δt_{ca} = 7-9 days) have characteristics similar to those reported immediately after comet Siding Spring's closest approach [*Gurnett et al.*, 2015], such as the one shown in Fig-

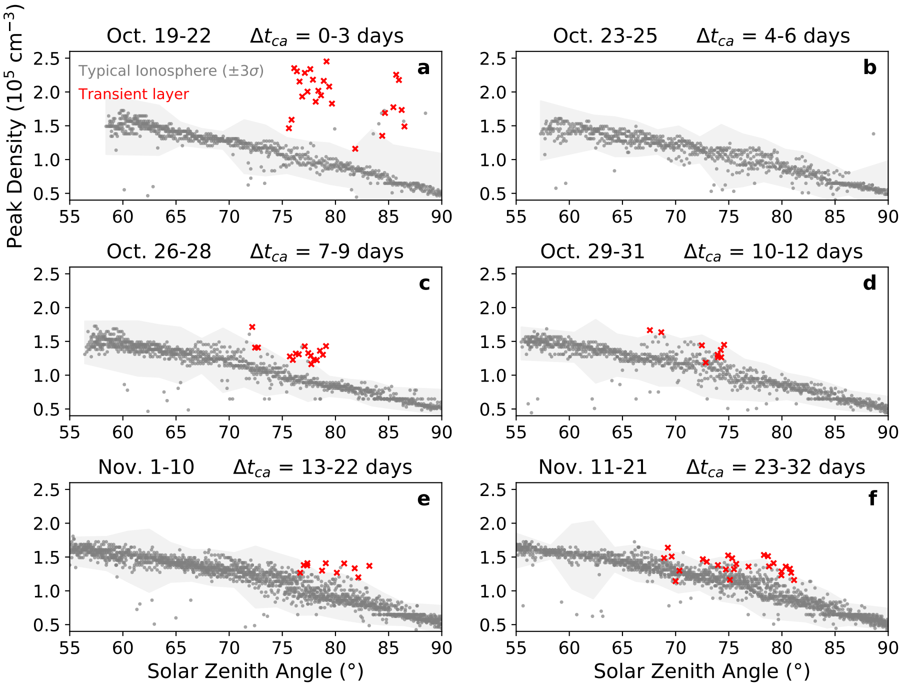

Figure 4. Each panel shows dayside peak densities as a function of solar zenith angle for a specified time period. The gray points are peak densities derived from normal ionospheric traces and the gray envelopes encompas detections the 3σ standard deviations in 2° SZA bins. The red crosses are the transient layer peak densities. The panel titles display the date ranges of the measurements and the time since comet Siding Spring's closest approach (Δt_{ca}).

ure 2b. These characteristics include an unusual reflection shape, a ground echo overlap, and extension to abnormally high frequencies. Most of the transient layer detections are located between 20°N-60°N latitude and 275°E to 95°E longitude, near the MAVEN IUVS observations obtained at Δt_{ca} = 1.0-2.5 days (Fig. 1). Nearly all of the transient layer peak electron densities are exceptionally high ($>3\sigma$) compared to the peak densities derived from typical ionospheric traces during the same time period (Fig. 4c). Together, these results make a compelling case for the transient layer lasting at least 7 days after closest approach, which is ~3.5 times longer than previously reported.

The transient layer reflections we identified between 29 October - 21 November (Δt_{ca} = 10-32 days) are from similar locations, but most of the peak densities are not 3σ outliers over the average peak densities of the normal ionosphere (Fig. 4d-f). However, during all three periods, the transient layer peak densities are mostly 1σ higher. This suggests that the transient layer may have lasted up to 32 days after closest approach, and the peak density decayed with time. The prolonged lifetime of the transient Mg^+ layer is perhaps not surprising given that metallic ion species can have long chemical lifetimes of a week or longer [*Whalley and Plane*, 2010; *Grebowsky et al.*, 2017]. However, there is currently no comprehensive time-dependent model of the Siding Spring event that allows us to compare our observed transient layer lifetime with predictions.

Despite detecting the transient layer up to 32 days after closest approach, we did not detect it continuously; no transient layer could be identified between 4-6 days after closest approach (23-25 October). This lack of detection is perplexing because the MARSIS instrument had similar observational coverage during the entirety of the 32 days we examined. One possible explanation is that the transient layer peak moved upwards and merged with the main peak of the ionosphere. This would cause the transient layer reflection and main ionospheric trace to be indistinguishable in ionograms. A second possible explanation is that the transient layer was so localized in longitude that MARSIS was unable to observe the right location during this period. A third possible explanation is that, by this time, the transient layer peak density had decayed to a value smaller than the peak density of the main ionosphere, preventing MARSIS from detecting the transient layer.

If the third explanation is true and the transient layer did decay between 23-25 October, then what caused it to come back? The flyby of comet Siding Spring coincidentally took place during a time of intense space weather [*Sánchez-Cano et al.*, 2018] when there were multiple active flare regions on the Sun. One of these regions, AR 12192, produced multiple X-class flares directed towards Mars as shown in Figure 5 [*Xu et al.*, 2018; *Fang et al.*, 2019]. It is known that solar flares increase the X-ray and extreme ultraviolet (EUV) photon flux, which leads to increased O_2^+ and electron densities, especially below the main peak of the ionosphere [*Mendillo et al.*, 2006; *Lollo et al.*, 2012; *Fallows et al.*, 2015; *Xu et al.*, 2018; *Thirupathaiah et al.*, 2019]. The increased densities below the main peak could potentially lead to ionogram features similar to those we identified as the transient layer. However, these false detections are unlikely because, at these altitudes, ionospheric plasma is composed primarily of NO^+ and O_2^+ [*Fox*, 2004], which rapidly recombine on timescales of minutes after a flare ends [*Fang et al.*, 2019].

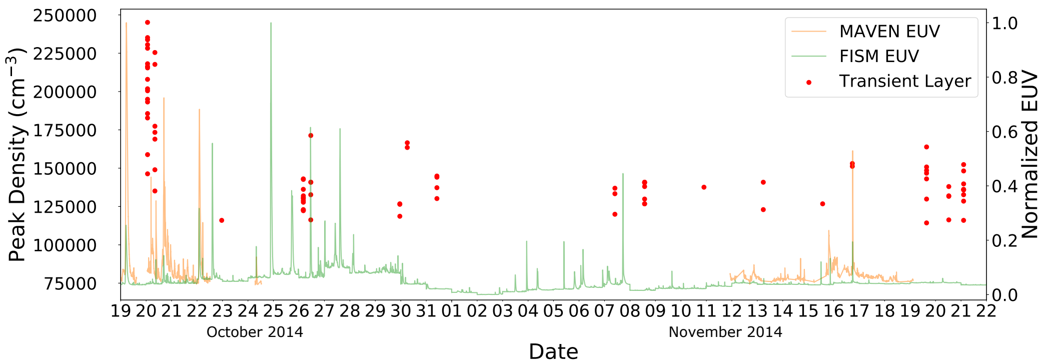

Figure 5. Transient layer detections during 20 October - 22 November, plotted with two solar extreme ultraviolet (EUV) irradiance datasets for reference. The irradiances are normalized relative to their maximum values during the period considered. The red data points indicate the transient layer detections. Orange data are MAVEN Extreme Ultraviolet Monitor measurements in the 0.1-7 nm wavelength range [*Eparvier et al.*, 2015]. Green data are from the Earth-based Flare Irradiance Spectral Model (FISM) [*Chamberlin et al.*, 2008]. During this period the Mars-Sun-Earth angle was ~90°.

Alternatively, if neutral Mg from the comet was still present in the upper atmosphere, then Mg^+ would be produced through charge exchange between Mg and O_2^+ ($Mg + O_2^+ \rightarrow Mg^+ + O_2$), which is the major chemical pathway for Mg^+ production [*Whalley and Plane*, 2010; *Plane et al.*, 2018]. The long lifetime of Mg^+ would allow MARSIS to detect the transient layer well after a flare occurred. This hypothesis requires Mg to be present in the upper atmosphere long after Siding Spring's closest approach. This may be possible, although current Mg^+ chemistry suggests that the buildup of Mg is limited [*Plane et al.*, 2018]. However, without detailed modeling that is out of the scope of this work, it is unclear how long Mg was present in the upper atmosphere after closest approach. Thus, this hypothesis is potentially possible.

Another possibility is that the transient layer we detect is created by a different mechanism proposed in *Crismani et al.* [2019]. In this mechanism, a sporadic layer is produced when the interplanetary magnetic field (IMF) is radial, allowing direct access of solar wind protons to the upper atmosphere. Ionization by precipitating solar wind protons can create a sporadic ionospheric layer below the main peak of the ionosphere.

This mechanism is also not global, but acts to enhance the electron density in a small region of the planet. Thus, this mechanism would also create localized enhancements of electron density, similar to what we observe. However, nearly all observations of a sporadic layer so far have a peak density much smaller than the main peak density and thus could not be observed by MARSIS [*Pätzold et al.*, 2005; *Withers et al.*, 2008]. Furthermore, it would be quite a coincidence if this mechanism was causing enhanced ionization in the same locations as the Siding Spring Mg^+ layer.

A final possibility is that a meteor shower unrelated to Siding Spring happened some time after closest approach. In general, this seems like a very unlikely possibility given that no meteor showers at Mars were predicted to occur during the month following closest approach [*Christou*, 2010; *Vaubaillon et al.*, 2014].

5 Conclusions

We have presented MARSIS observations that suggest the transient Mg^+ layer produced by comet Siding Spring's encounter with Mars lasted at least 7 days, and potentially up to 32 days. This is longer than reported by previous studies, which suggested the layer lasted ~1-2 days. The intense space weather during and after closest approached may have played a role in the prolonged lifetime of the transient layer. However, global simulations are needed to fully untangle the mechanisms that caused the transient layer to be localized and patchy for a prolonged period of time.

Table 1: Characteristics of the 86 transient layer measurements we identified in MARSIS ionograms. The columns list the date, time, MEX orbit number, East longitude (LON, °), latitude (LAT, °), solar zenith angle (SZA, °), peak electron density (N_{max}, 10^5 cm^{-3}), the crustal magnetic field strength at 400 km (B_{crust}, nT), and the angle between the magnetic field and the vertical direction (θ_{elev}, degrees).

Date	UT	Orbit	LON	LAT	SZA	N_{max}	B_{crust}	θ_{elev}
2014-10-20	1:19:32	13710	30.0	48.0	79.7	1.83	14.1	33.4
2014-10-20	1:19:40	13710	30.0	47.5	79.4	2.08	13.8	35.5
2014-10-20	1:19:47	13710	30.1	47.0	79.2	2.45	13.0	34.8
2014-10-20	1:19:55	13710	30.1	46.5	78.9	2.16	11.9	30.6
2014-10-20	1:20:02	13710	30.1	46.0	78.6	1.95	10.7	21.5
2014-10-20	1:20:10	13710	30.1	45.6	78.4	2.02	9.5	7.9
2014-10-20	1:20:17	13710	30.2	45.1	78.1	1.86	8.9	8.6
2014-10-20	1:20:25	13710	30.2	44.6	77.9	2.18	8.9	24.4
2014-10-20	1:20:32	13710	30.2	44.1	77.6	2.34	9.3	34.5
2014-10-20	1:20:40	13710	30.2	43.6	77.4	2.01	10.1	37.5
2014-10-20	1:20:47	13710	30.2	43.1	77.1	2.28	10.9	35.6
2014-10-20	1:20:55	13710	30.3	42.6	76.9	1.93	11.7	31.8
2014-10-20	1:21:03	13710	30.3	42.2	76.6	2.15	12.9	28.2
2014-10-20	1:21:10	13710	30.3	41.7	76.4	2.31	14.4	25.9
2014-10-20	1:21:18	13710	30.3	41.2	76.1	2.35	16.2	25.7
2014-10-20	1:21:25	13710	30.3	40.7	75.9	1.59	18.1	26.6
2014-10-20	1:21:33	13710	30.3	40.2	75.6	1.46	19.8	28.6
2014-10-20	8:15:50	13711	286.5	60.6	86.5	1.49	5.5	26.3
2014-10-20	8:15:57	13711	286.6	60.1	86.2	1.73	5.2	19.5
2014-10-20	8:16:05	13711	286.7	59.6	86.0	2.18	5.0	12.3
2014-10-20	8:16:13	13711	286.7	59.2	85.7	2.25	4.7	4.6
2014-10-20	8:16:20	13711	286.8	58.7	85.4	1.77	4.5	3.9
2014-10-20	8:16:43	13711	287.0	57.3	84.7	1.69	4.2	29.4
2014-10-20	8:16:50	13711	287.0	56.8	84.4	1.35	4.2	37.3
2014-10-22	23:13:39	13720	87.2	52.7	81.9	1.16	5.2	22.1
2014-10-26	4:09:42	13731	42.7	48.8	79.1	1.43	36.4	68.3
2014-10-26	4:09:50	13731	42.7	48.3	78.8	1.3	39.1	72.8
2014-10-26	4:09:57	13731	42.8	47.8	78.5	1.36	41.1	77.9
2014-10-26	4:10:05	13731	42.8	47.4	78.2	1.22	41.8	82.3
2014-10-26	4:10:12	13731	42.8	46.9	78.0	1.23	41.1	82.4
2014-10-26	4:10:20	13731	42.8	46.4	77.7	1.29	38.9	77.3
2014-10-26	4:10:35	13731	42.9	45.4	77.1	1.43	31.5	63.1
2014-10-26	4:10:50	13731	42.9	44.4	76.6	1.31	23.0	48.1
2014-10-26	4:10:58	13731	42.9	44.0	76.3	1.32	19.3	40.8
2014-10-26	4:11:05	13731	43.0	43.5	76.0	1.23	16.3	34.2
2014-10-26	4:11:13	13731	43.0	43.0	75.7	1.28	13.9	28.6
2014-10-26	11:09:53	13732	300.6	46.6	77.7	1.16	4.6	39.3
2014-10-26	11:10:01	13732	300.6	46.1	77.4	1.33	5.2	43.4
2014-10-26	11:12:09	13732	300.9	37.9	72.7	1.41	9.2	54.9
2014-10-26	11:12:17	13732	300.9	37.4	72.4	1.41	10.1	56.4
2014-10-26	11:12:24	13732	300.9	36.9	72.2	1.71	11.4	58.3
2014-10-29	23:05:41	13744	153.7	42.0	74.3	1.26	2.7	78.8
2014-10-29	23:05:48	13744	153.7	41.5	74.0	1.27	2.7	80.4
2014-10-29	23:06:18	13744	153.8	39.6	72.8	1.19	2.8	81.2
2014-10-30	6:07:40	13745	51.7	32.6	68.6	1.63	37.3	31.3
2014-10-30	6:08:10	13745	51.7	30.8	67.6	1.67	50.4	28.0
2014-10-31	10:03:06	13749	2.4	42.9	74.6	1.45	31.9	1.9
2014-10-31	10:03:13	13749	2.5	42.4	74.2	1.37	36.2	8.6

Table 1: Characteristics of the 86 transient layer measurements we identified in MARSIS ionograms. The columns list the date, time, MEX orbit number, East longitude (LON, °), latitude (LAT, °), solar zenith angle (SZA, °), peak electron density (N_{max}, 10^5 cm^{-3}), the crustal magnetic field strength at 400 km ($B_{\rm crust}$, nT), and the angle between the magnetic field and the vertical direction (θ_{elev}, degrees).

Date	UT	Orbit	LON	LAT	SZA	N_{max}	$B_{\rm crust}$	θ_{elev}
2014-10-31	10:03:21	13749	2.5	41.9	74.0	1.3	41.1	15.9
2014-10-31	10:03:58	13749	2.6	39.5	72.5	1.44	65.6	54.6
2014-11-07	9:48:23	13773	67.5	57.1	83.2	1.37	15.0	24.8
2014-11-07	9:48:45	13773	67.6	55.6	82.2	1.2	17.0	43.0
2014-11-07	9:48:53	13773	67.7	55.2	81.8	1.33	17.9	48.1
2014-11-08	13:47:19	13777	18.8	53.9	80.8	1.4	8.4	10.3
2014-11-08	13:47:34	13777	18.9	53.0	80.1	1.27	9.5	12.8
2014-11-08	13:47:57	13777	19.0	51.5	79.1	1.41	10.4	1.9
2014-11-08	13:48:05	13777	19.0	51.0	78.7	1.3	10.5	10.8
2014-11-08	13:48:35	13777	19.1	49.1	77.4	1.41	11.7	51.7
2014-11-08	13:48:42	13777	19.2	48.6	77.0	1.38	12.1	58.8
2014-11-08	13:48:50	13777	19.2	48.2	76.7	1.27	12.4	63.4
2014-11-10	21:44:48	13785	281.1	49.5	77.3	1.38	2.6	43.9
2014-11-13	5:39:47	13793	182.9	53.3	80.0	1.23	10.1	9.4
2014-11-13	5:40:02	13793	183.0	52.3	79.2	1.41	12.3	23.2
2014-11-15	13:35:26	13801	84.9	54.7	80.9	1.27	8.1	55.4
2014-11-16	17:34:07	13805	36.1	52.1	78.7	1.51	37.3	72.1
2014-11-16	17:34:15	13805	36.2	51.6	78.3	1.53	39.6	76.8
2014-11-19	15:31:05	13815	94.1	45.2	72.9	1.43	3.7	66.4
2014-11-19	15:31:13	13815	94.1	44.7	72.6	1.47	3.7	68.7
2014-11-19	15:31:58	13815	94.2	41.9	70.4	1.3	3.8	74.6
2014-11-19	15:32:05	13815	94.2	41.5	70.0	1.14	3.7	74.4
2014-11-19	15:32:13	13815	94.2	41.0	69.6	1.51	3.7	74.1
2014-11-19	15:32:20	13815	94.3	40.6	69.3	1.64	3.6	73.7
2014-11-19	15:32:28	13815	94.3	40.1	68.9	1.49	3.5	73.0
2014-11-20	12:28:45	13818	147.2	48.5	75.5	1.32	2.4	35.1
2014-11-20	12:28:52	13818	147.2	48.0	75.1	1.16	2.2	38.7
2014-11-20	12:29:00	13818	147.2	47.6	74.7	1.32	2.1	43.0
2014-11-20	12:29:15	13818	147.3	46.6	74.0	1.38	2.0	53.3
2014-11-21	2:25:57	13820	302.2	55.5	81.1	1.16	2.2	28.9
2014-11-21	2:26:04	13820	302.2	55.0	80.8	1.33	2.4	36.4
2014-11-21	2:26:12	13820	302.3	54.5	80.4	1.36	2.5	41.4
2014-11-21	2:26:19	13820	302.3	54.1	80.0	1.28	2.6	44.0
2014-11-21	2:26:42	13820	302.4	52.6	78.8	1.36	2.4	38.5
2014-11-21	2:27:20	13820	302.6	50.3	76.9	1.36	1.5	28.9
2014-11-21	2:27:42	13820	302.7	48.8	75.7	1.4	3.2	37.9
2014-11-21	2:27:50	13820	302.7	48.4	75.3	1.48	4.0	38.5
2014-11-21	2:27:57	13820	302.8	47.9	74.9	1.52	4.8	39.6

Acknowledgments

All the MARSIS data used in this study are publicly available at `https://space.physics.uiowa.edu/marsx/public-data.html`. MAVEN EUV data can be found at `https://lasp.colorado.edu/maven/sdc/public/pages/datasets/euv.html`. MAVEN FISM EUV data, produced by the Laboratory for Atmospheric and Space Physics (LASP) can be found at `http://lasp.colorado.edu/lisird/`. The research at the University of

Iowa was supported by NASA through contract 1224107 with the Jet Propulsion Laboratory. We thank the many members of the scientific, technical, and management teams at NASA Headquarters, the Jet Propulsion Laboratory, the European Space Agency, and the Italian Space Agency for their efforts in planning the spacecraft operations required to successfully obtain these data. We thank Bill Kurth, Hadi Madanian, John Plane, and Matteo Crismani for their insightful discussions on the topic. We give special thanks to Chris Piker for helping with data acquisition using the das2py software package (`https://das2.org/das2py/`) and to Larry Granroth who provided useful programs for analyzing MARSIS data. Additionally, we thank Thomas Koeppel for his dedicated administrative work during Z. Luppen's time at the University of Iowa.

References

Benna, M., P. R. Mahaffy, J. M. Grebowsky, J. M. C. Plane, R. V. Yelle, and B. M. Jakosky (2015), Metallic ions in the upper atmosphere of Mars from the passage of comet C/2013 A1 (Siding Spring), *Geophys. Res. Lett.*, *42*, 4670–4675, doi:10.1002/2015GL064159.

Chamberlin, P. C., T. N. Woods, and F. G. Eparvier (2008), Flare Irradiance Spectral Model (FISM): Flare component algorithms and results, *Space Weather*, *6*, S05001, 10.1029/2007SW000372, doi:10.1029/2007SW000372.

Christou, A. A. (2010), Annual meteor showers at venus and mars: lessons from the earth, *Mon. Not. R. Astron. Soc.*, *402*(4), 2759–2770, doi:10.1111/j.1365-2966.2009.16097.x.

Crismani, M. M. J., N. M. Schneider, J. M. C. Plane, J. S. Evans, S. K. Jain, M. S. Chaffin, J. D. Carrillo-Sanchez, J. I. Deighan, R. V. Yelle, A. I. F. Stewart, W. McClintock, J. Clarke, G. M. Holsclaw, A. Stiepen, F. Montmessin, and B. M. Jakosky (2017), Detection of a persistent meteoric metal layer in the Martian atmosphere, *Nat. Geosci.*, *10*(6), 401–404, doi:10.1038/ngeo2958.

Crismani, M. M. J., N. M. Schneider, J. S. Evans, J. M. C. Plane, J. D. Carrillo-Sánchez, S. Jain, J. Deighan, and R. Yelle (2018), The Impact of Comet Siding Spring's Meteors on the Martian Atmosphere and Ionosphere, *J. Geophys. Res.*, *123*(10), 2613–2627, doi: 10.1029/2018JE005750.

Crismani, M. M. J., J. Deighan, N. M. Schneider, J. M. C. Plane, P. Withers, J. Halekas, M. Chaffin, and S. Jain (2019), Localized ionization hypothesis for transient ionospheric layers, *J. Geophys. Res.*, *124*(6), 4870–4880, doi:10.1029/2018JA026251.

Duru, F., D. A. Gurnett, D. D. Morgan, R. Modolo, A. F. Nagy, and D. Najib (2008), Electron densities in the upper ionosphere of mars from the excitation of electron plasma oscillations, *J. Geophys. Res.*, *113*, A07302, doi:10.1029/2008JA013073.

Duru, F., D. D. Morgan, and D. A. Gurnett (2010), Overlapping ionospheric and surface echoes observed by the Mars Express radar sounder near the Martian terminator, *Geophys. Res. Lett.*, *37*(23), L23102, doi:10.1029/2010GL045859.

Eparvier, F. G., P. C. Chamberlin, T. N. Woods, and E. M. B. Thiemann (2015), The Solar Extreme Ultraviolet Monitor for MAVEN, *Space Sci. Rev.*, *195*, 293–301, doi:10.1007/s11214-015-0195-2.

Espley, J. R., G. A. DiBraccio, J. E. P. Connerney, D. Brain, J. Gruesbeck, Y. Soobiah, J. Halekas, M. Combi, J. Luhmann, Y. Ma, Y. Jia, and B. Jakosky (2015), A comet engulfs mars: Maven observations of comet siding spring's influence on the martian magnetosphere, *Geophys. Res. Lett.*, *42*(21), 8810–8818, doi:10.1002/2015GL066300.

Fallows, K., P. Withers, and G. Gonzalez (2015), Response of the Mars ionosphere to solar flares: Analysis of MGS radio occultation data, *J. Geophys. Res.*, *120*(11), 9805–9825, doi:10.1002/2015JA021108.

Fallows, K., P. Withers, D. Morgan, and A. Kopf (2019), Extremely high plasma densities in the mars ionosphere associated with cusp-like magnetic fields, *J. Geophys. Res.*, *124*(7), 6029–6046, doi:10.1029/2019JA026690.

Fang, X., D. Pawlowski, Y. Ma, S. Bougher, E. Thiemann, F. Eparvier, W. Wang, C. Dong, C. O. Lee, Y. Dong, M. Benna, M. Elrod, P. Chamberlin, P. Mahaffy, and B. Jakosky

(2019), Mars Upper Atmospheric Responses to the 10 September 2017 Solar Flare: A Global, Time-Dependent Simulation, *Geophys. Res. Lett.*, *46*(16), 9334–9343, doi: 10.1029/2019GL084515.

Fox, J. L. (2004), Response of the martian thermosphere/ionosphere to enhanced fluxes of solar soft x rays, *J. Geophys. Res.*, *109*, A11310, doi:10.1029/2004JA010380.

Grebowsky, J. M., M. Benna, J. M. C. Plane, G. A. Collinson, P. R. Mahaffy, and B. M. Jakosky (2017), Unique, non-earthlike, meteoritic ion behavior in upper atmosphere of mars, *Geophys. Res. Lett.*, *44*(7), 3066–3072, doi:10.1002/2017GL072635.

Gurnett, D. A., D. L. Kirchner, R. L. Huff, D. D. Morgan, A. M. Persoon, T. F. Averkamp, F. Duru, E. Nielsen, A. Safaeinili, J. J. Plaut, and G. Picardi (2005), Radar soundings of the ionosphere of Mars, *Science*, *310*, 1929–1933, doi:10.1126/science.1121868.

Gurnett, D. A., R. L. Huff, D. D. Morgan, A. M. Persoon, T. F. Averkamp, D. L. Kirchner, F. Duru, F. Akalin, A. J. Kopf, E. Nielsen, A. Safaeinili, J. J. Plaut, and G. Picardi (2008), An overview of radar soundings of the martian ionosphere from the Mars Express spacecraft, *Adv. Space Res.*, *41*, 1335–1346, doi:10.1016/j.asr.2007.01.062.

Gurnett, D. A., D. D. Morgan, A. M. Persoon, L. J. Granroth, A. J. Kopf, J. J. Plaut, and J. L. Green (2015), An ionized layer in the upper atmosphere of Mars caused by dust impacts from comet Siding Spring, *Geophys. Res. Lett.*, *42*(12), 4745–4751, doi:10.1002/2015GL063726.

Kopf, A. J., D. A. Gurnett, D. D. Morgan, and D. L. Kirchner (2008), Transient layers in the topside ionosphere of mars, *Geophys. Res. Lett.*, *35*, L17102, doi:10.1029/2008GL034948.

Lollo, A., P. Withers, K. Fallows, Z. Girazian, M. Matta, and P. C. Chamberlin (2012), Numerical simulations of the ionosphere of Mars during a solar flare, *J. Geophys. Res.*, *117*(A5), doi:10.1029/2011JA017399.

Mendillo, M., P. Withers, D. Hinson, H. Rishbeth, and B. Reinisch (2006), Effects of Solar Flares on the Ionosphere of Mars, *Science*, *311*(5764), 1135–1138, doi:10.1126/science.1122099.

Morgan, D. D., D. A. Gurnett, D. L. Kirchner, J. L. Fox, E. Nielsen, and J. J. Plaut (2008), Variation of the martian ionospheric electron density from Mars Express radar soundings, *J. Geophys. Res.*, *113*, A09303, doi:10.1029/2008JA013313.

Morschhauser, A., V. Lesur, and M. Grott (2014), A spherical harmonic model of the lithospheric magnetic field of Mars, *J. Geophys. Res.*, *119*, 1162–1188, doi:10.1002/2013JE004555.

Pätzold, M., S. Tellmann, B. Häusler, D. Hinson, R. Schaa, and G. L. Tyler (2005), A sporadic third layer in the ionosphere of Mars, *Science*, *310*, 837–839, doi:10.1126/science.1117755.

Picardi, G., D. Biccari, R. Seu, J. Plaut, W. T. K. Johnson, R. L. Jordan, A. Safaeinili, D. A. Gurnett, R. Huff, R. Orosei, O. Bombaci, D. Calabrese, and E. Zampolini (2004), *MARSIS: Mars Advanced Radar for Subsurface and Ionosphere Sounding*, pp. 51–69, ESA SP-1240: Mars Express: the Scientific Payload, available online at http://sci.esa.int/science-e/www/object/index.cfm?fobjectid=34885.

Plane, J. M. C., J. D. Carrillo-Sanchez, T. P. Mangan, M. M. J. Crismani, N. M. Schneider, and A. Määttänen (2018), Meteoric metal chemistry in the martian atmosphere, *Journal of Geophysical Research: Planets*, *123*(3), 695–707, doi:10.1002/2017JE005510.

Restano, M., J. J. Plaut, B. A. Campbell, Y. Gim, D. Nunes, F. Bernardini, A. Egan, R. Seu, and R. J. Phillips (2015), Effects of the passage of Comet C/2013 A1 (Siding Spring) observed by the Shallow Radar (SHARAD) on Mars Reconnaissance Orbiter, *Geophys. Res. Lett.*, *42*(12), 4663–4669, doi:10.1002/2015GL064150.

Sánchez-Cano, B., O. Witasse, M. Lester, A. Rahmati, R. Ambrosi, R. Lillis, F. Leblanc, P.-L. Blelly, M. Costa, S. W. H. Cowley, J. R. Espley, S. E. Milan, J. J. Plaut, C. Lee, and D. Larson (2018), Energetic particle showers over mars from comet c/2013 a1 siding spring, *J. Geophys. Res.*, *123*(10), 8778–8796, doi:10.1029/2018JA025454.

Sánchez-Cano, B., O. Witasse, M. Lester, A. Rahmati, R. Ambrosi, R. Lillis, F. Leblanc, P.-L. Blelly, M. Costa, S. W. H. Cowley, J. R. Espley, S. E. Milan, J. J. Plaut, C. Lee, and

D. Larson (2018), Energetic Particle Showers Over Mars from Comet C/2013 A1 Siding Spring, *J. Geophys. Res.*, *123*(10), 8778–8796, doi:10.1029/2018JA025454.

Sánchez-Cano, B., M. Lester, O. Witasse, D. D. Morgan, H. Opgenoorth, D. J. Andrews, P.-L. Blelly, S. W. H. Cowley, A. J. Kopf, F. Leblanc, J. R. Espley, and A. Cardesín-Moinelo (2020), Mars' ionospheric interaction with comet c/2013 a1 siding spring's coma at their closest approach as seen by mars express, *J. Geophys. Res.*, *125*(1), e2019JA027,344, doi: 10.1029/2019JA027344.

Schneider, N. M., J. I. Deighan, A. I. F. Stewart, W. E. McClintock, S. K. Jain, M. S. Chaffin, A. Stiepen, M. Crismani, J. M. C. Plane, J. D. Carrillo-Sánchez, J. S. Evans, M. H. Stevens, R. V. Yelle, J. T. Clarke, G. M. Holsclaw, F. Montmessin, and B. M. Jakosky (2015), MAVEN IUVS observations of the aftermath of the Comet Siding Spring meteor shower on Mars, *Geophys. Res. Lett.*, *42*(12), 4755–4761, doi:10.1002/2015GL063863.

Thirupathaiah, P., S. Y. Shah, and S. Haider (2019), Characteristics of solar x-ray flares and their effects on the ionosphere and human exploration to mars: Mgs radio science observations, *Icarus*, *330*, 60 – 74, doi:https://doi.org/10.1016/j.icarus.2019.04.015.

Vaubaillon, J., L. Maquet, and R. Soja (2014), Meteor hurricane at Mars on 2014 October 19 from comet C/2013 A1, *Mon. Not. R. Astron. Soc.*, *439*(4), 3294–3299, doi:10.1093/mnras/stu160.

Venkateswara Rao, N., P. ManasaMohana, A. Jayaraman, and S. V. B. Rao (2016), Some new aspects of the transient ionization layer of comet Siding Spring origin in the Martian upper atmosphere, *J. Geophys. Res.*, *121*(4), 3592–3602, doi:10.1002/2015JA022189.

Wang, X. D., J. S. Wang, E. Nielsen, and H. Zou (2009), "Hook" structure in MARSIS ionogram and its interpretation, *Geophys. Res. Lett.*, *36*(13), L13103, doi:10.1029/2009GL038844.

Whalley, C. L., and J. M. C. Plane (2010), Meteoric ion layers in the Martian atmosphere, *Faraday Discuss.*, *147*, 349, doi:10.1039/c003726e.

Witasse, O., B. SÃąnchez-Cano, M. L. Mays, P. KajdiÄŊ, H. Opgenoorth, H. A. Elliott, I. G. Richardson, I. Zouganelis, J. Zender, R. F. Wimmer-Schweingruber, L. Turc, M. G. G. T. Taylor, E. Roussos, A. Rouillard, I. Richter, J. D. Richardson, R. Ramstad, G. Provan, A. Posner, J. J. Plaut, D. Odstrcil, H. Nilsson, P. Niemenen, S. E. Milan, K. Mandt, H. Lohf, M. Lester, J.-P. Lebreton, E. Kuulkers, N. Krupp, C. Koenders, M. K. James, D. Intzekara, M. Holmstrom, D. M. Hassler, B. E. S. Hall, J. Guo, R. Goldstein, C. Goetz, K. H. Glassmeier, V. GÃĺnot, H. Evans, J. Espley, N. J. T. Edberg, M. Dougherty, S. W. H. Cowley, J. Burch, E. Behar, S. Barabash, D. J. Andrews, and N. Altobelli (2017), Interplanetary coronal mass ejection observed at STEREO-A, Mars, comet 67P/Churyumov-Gerasimenko, Saturn, and New Horizons en route to Pluto: Comparison of its Forbush decreases at 1.4, 3.1, and 9.9 AU, *J. Geophys. Res.*, *122*(8), 7865–7890, doi:10.1002/2017JA023884.

Withers, P. (2009), A review of observed variability in the dayside ionosphere of Mars, *Adv. Space Res.*, *44*, 277–307, doi:10.1016/j.asr.2009.04.027.

Withers, P., M. Mendillo, D. P. Hinson, and K. Cahoy (2008), Physical characteristics and occurrence rates of meteoric plasma layers detected in the martian ionosphere by the mars global surveyor radio science experiment, *J. Geophys. Res.*, *113*, A12314, doi:10.1029/2008JA013636.

Xu, S., E. Thiemann, D. Mitchell, F. Eparvier, D. Pawlowski, M. Benna, L. Andersson, M. W. Liemohn, S. Bougher, and C. Mazelle (2018), Observations and Modeling of the Mars Low-Altitude Ionospheric Response to the 10 September 2017 X-Class Solar Flare, *Geophys. Res. Lett.*, *45*(15), 7382–7390, doi:10.1029/2018GL078524.